

RATIONAL PUMPING SYSTEM FOR HIGH-POWER INDUSTRIAL CO₂ LASER

Vladimir G.Niziev, Vladislav Ya.Panchenko

NICTL-Laser Research Center, Russian Academy of Sciences,
Shatura, Moscow Region, 140700, RUSSIA

ABSTRACT

Our original pumping system for the gas-discharge TE CO₂-laser was tested in the 5 kW laser. It includes crossed electrodes (20 anodes, 5 cathodes), thyristor inverter (2.5 kHz), system of unballast connections of sections to the inverter. The preionizer placed upstream realizes the 100 kHz discharge through dielectric electrodes. On the basis of the principle of minimum of energy dissipation high efficiency of current distribution over crossings (20×5) with a small number of sections (20+5) is shown. It provides a stable DC discharge at average power input to 4W/cm³ due to influence of upstream discharges upon the downstream ones.

The active medium of the laser was studied by method of IR luminescence at the wavelength 2-8 μm in "switched on" and "switched off" resonator. The luminescence intensity in the band 4.3 μm gives the particular information about the active medium. The 2D model of a discharge segmented along the gas flow was constructed to describe the distribution of electrical, gas-dynamic and kinetic characteristics. It was shown that in the most volume of chamber the discharge burns in the recombining plasma at reduced E/n, thus favoring high excitation efficiency.

Keywords: pumping system, gas discharge, discharge stability, gas discharge laser

2. INTRODUCTION

The gas-discharge convectively-cooled CO₂-lasers are known to rank high among the technological-purpose lasers. The prospects for wide commercial application of high-power industrial lasers are connected with the reduction of specific cost to 25-50 \$/W. Recently 20 kW and 40 kW FAF-lasers with HF excitation were developed¹. The price of these state-of-the-art models using complicated and expensive technical decisions exceeds 150 \$/W. It accords with the predictions,² where a conclusion about much higher cost of HF conception than DC was made on the basis of direct analysis of these two approaches.

The most powerful technological lasers are created according to the conception of TE-lasers with DC pumping system because of their low price and high reliability. Here they use sectionalized electrodes to spread discharge over the whole gas discharge chamber. Practically they use only one of the simplest techniques of electrodes sectionalization: each section is connected with the power supply through the active ballast resistors³⁻⁵. This lowers the laser efficiency and gives rise to technical problems of the released heat removal from the ballast resistors.

It was difficult to find a more rational technical decision because up to now there was not any theory for estimating the stability of discharges with multi-sectionalized electrodes and the efficiency of such an electrode system as a unit. The present work formulates and solves just this very problem. As far as the sectionalized electrode system is concerned, one can speak of stability in two quite different senses, defining in the long run the discharge ultimate characteristics.

Firstly, it is the stability of an individual diffuse discharge burning, in view of the discharge contraction and transition to arc at the local excess of some ultimate value jE/p (j is the current density; E is the electric intensity; p is the pressure). A great number of papers deal with the problems of discharge burning stability in terms of non-sectionalized electrodes. Depending on the gas mixture composition and specific conditions, the authors propose a number of discharge instability progress mechanisms which limit the parameters of specific energy input.

Secondly, the stability of the total current distribution over the sections can be spoken about, the qualitative shape of the discharge (diffuse, for example) being preserved. Just this very stability is the subject of the present work. The fluctuations of current distribution over the sections are dependent on the environment inhomogeneity and on the stability of the total current distribution in the sections. Such external conditions, the inhomogeneity of which influences the energy characteristics and uniformity of the discharge, include, for example, accuracy of the electrode system fabrication, gas flow uniformity, oxidation of electrodes, depression zone formation, etc. Non-uniformities of this kind cause redistribution currents in the electrode system. As a result, in some regions energy release exceeds considerably the average value. When the chamber operates in power strength regimes, these regions turn out the "weakpoints" and cause typical instabilities, resulting subsequently in arcing. The specific energy input can be increased in particular by increasing the stability to possible current redistribution caused by the external conditions non-uniformity.

The present work studies the stability of the sectionalized discharge burning in the gas flow in the electrode system with the crossed electrodes, where the cathode is sectionalized along the gas flow direction and the anode across the direction of the flow. In such system the discharges should burn where the cathode and anode sections cross. The discharge high stability in the electrode system of this type is associated with the influence of the discharges occurring upstream on the downstream ones. This means that the downstream discharge gaps are influenced by the heated, partially ionized gas, its temperature and degree of ionization being determined by the energy input to the upstream discharge. The use of this electrode system gives a practical advantage of heavy sectionalizing with one-dimensional electrodes and is of interest from the physical viewpoint, too. The current distribution in the system can be calculated from the principle of energy dissipation minimum ⁶, the dissipation function second derivative with respect to the independent variables characterizes this distribution stability.

3. THEORY OF 2D CURRENT DISTRIBUTION STABILITY

Schematic arrangement of the electrodes in the gas and connections of the sections with the power supply for the calculated schemes are illustrated in Fig.1.

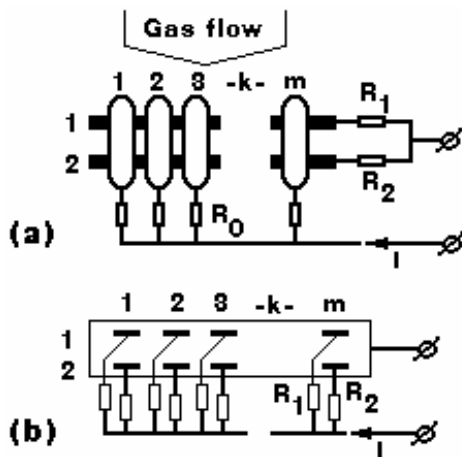


Fig. 1. Schematic arrangement of the electrodes in the gas flow and connections of sections with the power supply for two schematic situations: a) the diagram of crossed electrodes; b) the traditional scheme with the 2D sectionalized cathode.

Energy dissipation function for crossed electrodes Fig.1a is written as

$$W = \sum_{k=1}^m (U_{k,1} \cdot i_{k,1} + U_{k,2} \cdot i_{k,2}) + R_0 \cdot \sum_{k=1}^m (i_{k,1} + i_{k,2})^2 + R_1 \cdot (\sum_{k=1}^m i_{k,1})^2 + R_2 \cdot (\sum_{k=1}^m i_{k,2})^2 \quad (1)$$

where subscripts 1 and 2 refer to horizontal and subscript k to vertical electrode sections; U, i stand for voltage and current of individual discharges burning at the crossings. Let us consider the case with linear representation of each individual discharge volt-ampere characteristics (VAC):

$$U_{k,1} = \hat{U} + R \cdot i_{k,1} ; \quad U_{k,2} = \hat{U}_k + R \cdot i_{k,2} \quad (2)$$

According to this record, VAC of the discharges with subscripts k,1 are identical. As for the discharges with subscripts k,2, the dependence of the voltage on the current is general in its form. But due to the experimentally observed influence of the upstream discharges upon the downstream ones, the value of U decreases as a function of the energy input to the discharge with the subscript k,1. In the linear approximation

$$\hat{U}_k = \hat{U} \cdot (1 - \alpha \cdot U_{k,1} \cdot i_{k,1}) \approx \hat{U} \cdot (1 - \alpha \cdot \hat{U} \cdot i_{k,1}) \quad (3)$$

where α is the factor of the upstream discharge influence upon the downstream one.

The approximate expression is valid due to the small values of R in actual VAC of glow discharges. To calculate the current distribution, corresponding to function W conditional minimum of the expression (1) should be supplemented with the necessary conditions of connection. A complete set of conditions can be written according to Kirchoff's law for branched circuits. We must use the following "necessary conditions of connection" from the complete set to calculate the conditional minimum of the expression (1) :

$$\sum_{k=1}^m (i_{k,1} + i_{k,2}) = I; \quad U_{k,1} - U_{k,2} + U_{R1} - U_{R2} = 0, \quad k=1, 2 \dots m \quad (4)$$

where I is the total current; U_{R1} , U_{R2} stand for the voltage drops across the corresponding resistors.

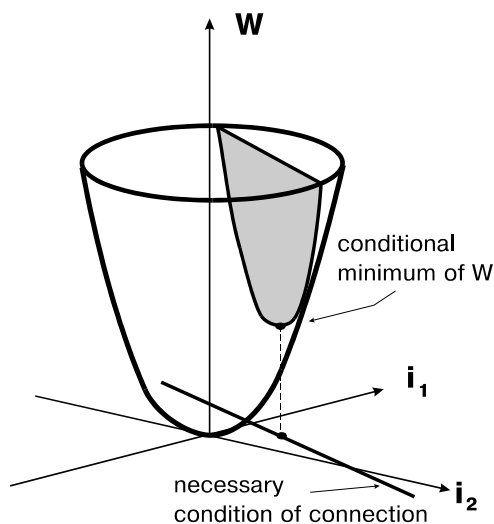


Fig.2. Illustration of search for solution of 2D situation.

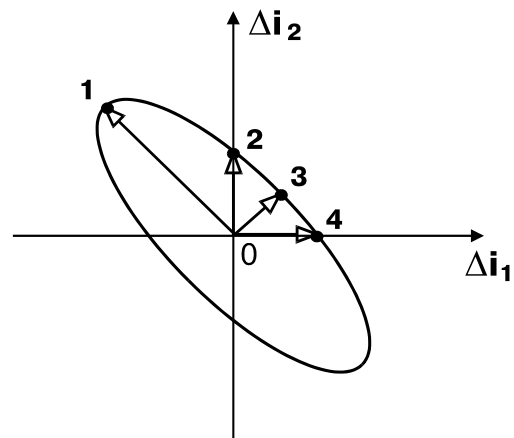


Fig.3. Schematic illustration of variations of discharge current distribution stability in different directions on the plane i_1 and i_2 . Minimum stability - point 1; maximum - point 3; the same values of stability in the directions 2 and 4.

Fig.2 illustrates schematically the search for solution of 2D situation and the "action" of necessary condition of connection in calculation of conditional minimum of function W. The distribution of currents which agrees with function (1) conditional minimum, in view of conditions (4) can be calculated by the method of Lagrange coefficients. The solution does not depend on the subscript k: $i_{k,1} = i_1$, $i_{k,2} = i_2$. Following the substitution $i_{k,j} = i_j + \Delta i_{k,j}$ in (1,4) and reducing the number of independent variables in accordance with (4), we have

$$W = W_d + W_b + [R_0 \cdot (2 + \beta)^2 + R \cdot (2 + \beta)] \cdot \sum_{q=p}^{m-1} \sum_{p=1}^{m-1} \zeta_{p,q} \cdot \Delta i_{p,1} \cdot \Delta i_{q,1} \quad (5)$$

W_d , W_b - are powers dissipated in the discharges and ballast resistors for currents in the discharges i_1 , i_2 .

$$\zeta_{p,q} = \begin{cases} 1 & p = q \\ 0.5 & p \neq q \end{cases}$$

The eigenvalues of the matrix of function W second derivatives with respect to Δi are as follows:

$$\lambda_1 = m; \quad \lambda_k = 1 \quad (k=2,3\dots m-1) \quad (6)$$

Following the determination of the eigenvectors and their orthogonalization, the identity matrix of the coordinates Δi transformation into the coordinates δ ($k=1,2\dots m-1$) can be set up for diagonalization of the square form (5) (Table 1).

Let's write (5) in the canonical form

$$W = W_d + W_b + 2 \cdot [R_0 \cdot (2 + \beta)^2 + R \cdot (2 + \beta)] \cdot \sum_{k=1}^{m-1} \lambda_k \cdot \delta_k^2 \quad (7)$$

For the multi-sectionalized discharge, the current fluctuation, disturbing the equilibrium of the system, is understood as optional linear combination $\Delta i_{k,1}$. The distribution stability (7) with respect to the fluctuation of such type is determined as the second derivative of W in m-1-dimensional space, in the direction determined by the form of the linear combination $\Delta i_{k,1}$ (see Fig.3).

The function W second derivative in this case has the dimensional representation of resistance and can be interpreted as the resistance included in the circuit of the given current fluctuation. As (7) proves, the current distribution stability for fluctuations of an arbitrary type has the maximum and minimum values corresponding to two values of λ_k .

$$2 [R_0 (2 + \beta)^2 + R (2 + \beta)] < R_{\text{eff}} < 2m [R_0 (2 + \beta)^2 + R (2 + \beta)] \quad (8)$$

The analysis of (8) proves that the stability of the current distribution in the system under consideration is determined not only by the resistance R_0 ; the influence of the upstream discharges on the downstream ones plays here a substantial role (the β -parameter).

Table 1

	δ_1	δ_2	δ_3	δ_{m-1}
$\Delta i_{1,1}$	$1 / \sqrt{(m-1)}$	$1 / \sqrt{2}$	$1 / \sqrt{6}$	$1 / \sqrt{(m-2) \cdot (m-1)}$
$\Delta i_{2,1}$	$1 / \sqrt{(m-1)}$	$-1 / \sqrt{2}$	$1 / \sqrt{6}$	$1 / \sqrt{(m-2) \cdot (m-1)}$
$\Delta i_{3,1}$	$1 / \sqrt{(m-1)}$	0	$-2 / \sqrt{6}$	$1 / \sqrt{(m-2) \cdot (m-1)}$
.....
$\Delta i_{m-1,1}$	$1 / \sqrt{(m-1)}$	0	0	$-(m-2) / \sqrt{(m-2) \cdot (m-1)}$

The further discussions will be concerned with the stability minimum value for the current fluctuations for which the algebraic sum of the currents deviations is equal to zero (see the Table 1).

The efficiencies of various electrode systems with the identical major integral characteristics of the discharge are shown in Fig.4. It can serve as the direct practical recommendations for the future successful applications of the crossed-electrode system. The stability of current distribution in this scheme is the highest at the same power dissipation in the discharge and ballast resistors.

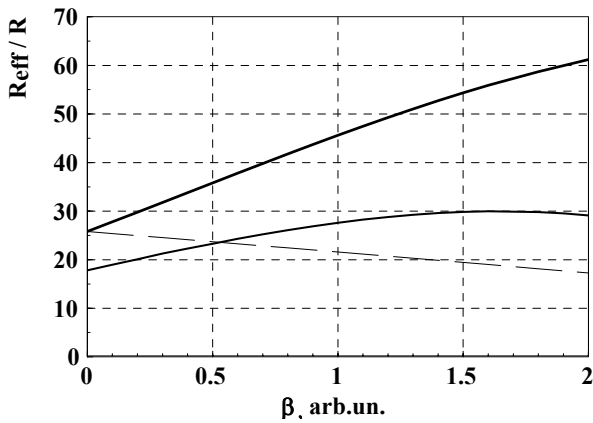


Fig. 4. R_{eff} dependencies on β under energy parameters are constant. The full thick curve is for crossed electrodes Fig.1a, $R_1 = 0.1 \text{ k}\Omega$. The full thin one is just the same at $R_1 = 0$. The dashed fall down dependence is for scheme Fig. 1b. For all curves $U = 3 \text{ kV}$, $R_0 = 1 \text{ k}\Omega$, $i_1 = i_2$, $W_d = 50 \text{ kW}$, $W_b = 30 \text{ kW}$.

Parameter β depends on the main characteristics of the discharge and gas flow:

$$\beta = \frac{\gamma - 1}{\gamma} \cdot \frac{(E/p)^2 \cdot p \cdot d}{r_0 \cdot V} \quad (8)$$

where γ is the adiabatic constant, V is the gas flow velocity; d is the interelectrode gap; r_0 is the differential resistance of the discharge referred to the discharge length unit.

The estimation for the typical values $\gamma \sim 1.4$, $E/p = 15 \text{ V/cm}\cdot\text{Torr}$, $p \cdot d = 120 \text{ Torr}\cdot\text{cm}$, $V = 100 \text{ m/s}$, $r_0 = 50 \text{ W}\cdot\text{m}$ gives $\beta = 1.15$.

4. EXPERIMENTAL SETUP

The flowing facility of the laser provides the gas flow rate 100 m/s in the discharge chamber having $6 \times 100 \text{ cm}^2$ section Fig.5. The anode sections are manufactured of 20 copper strips mounted on a single dielectric slab. The cathode sections, presented 6 copper tubes having 6 mm diameter are located inside the chamber. The spacing between the anode sections and the cathode tubes increases downstream from 5.5 to 6.5 cm. The preionizer is located upstream with respect to the electrode system. The special-purpose power source applies the sinusoidal 20-120kHz voltage to the preionizer electrodes. The discharge burns between the 2 quartz tube surfaces, the tubes having 11 mm outside diameter. The quartz tubes contain the water-cooled copper tubes. The preionizer discharge power reaches 2-3kW. The power source contains the inverter and the system of sections unballasted connection to the inverter. This system has high inner resistance and feeds the discharge by pulsed or continuous current.

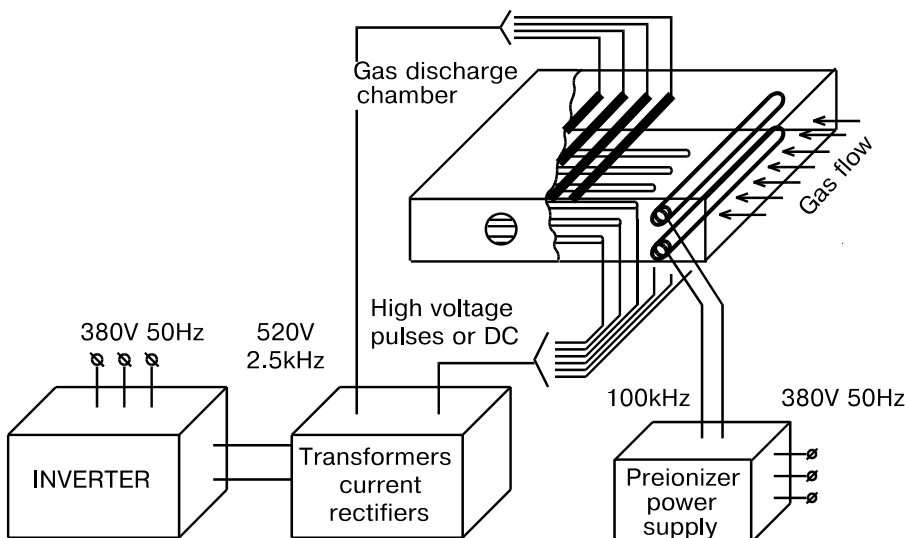


Fig.5. The block scheme of the pumping system.

This pumping system has a number of advantages. The power supply has small dimensions, the volume of the 50kW inverter is 0.35m³ and the system of sections unballasted connection has the volume 0.25m³. The power supply is characterized by high efficiency and relatively low operating voltage in view of the grounded midpoint feed circuit. The employed inverter has big inner resistance, which is optimum for powering the self-maintained discharges with weakly rising volt-ampere characteristics. The scheme solution with the connected in series primary windings of the transformers provides the "rigid distribution" of currents in the sections. The absence of active ballast increases 1.5 times the pumping system efficiency. The adjustment of the power in the discharge is executed by varying the inverter frequency.

Fig.6 presents the shape of the inverter current per resistive load at various frequency values. As the figure shows, two ranges of the inverter operating frequency exist: the pulsed regime at $f < f_0$ and the quasi continuous one at $f > f_0$. Fig.7 illustrates the stable-resonator laser beam power dependence on the inverter consumed power. Some more experimental characteristics of the work of such pumping system can be found in ⁷.

5. IR LUMINESCENCE DIAGNOSTIC OF ACTIVE MEDIUM

The uniformity of the discharge and the spatial distribution of the vibration-excited gas are the notable factors in view of the problem of laser beam quality and ultimate power achievement. When operating the laser, a two-dimensional field of discharges is generated in the volume of the gas-discharge chamber (GDC), its spatial structure being governed by the electrode system geometry, gas composition, energy input, flow rate, etc. So from the viewpoint of optical resonator choice and laser optimization by the energy parameters, it becomes important to study the topology of the discharge field in the GDC. It is also necessary to estimate the extent to which the level of vibrational excitation of the working gas CO₂ is uniform, as it has a determining effect on the uniformity of the amplification factor in the chamber volume.

The method based on registration of IR luminescence of gas mixture molecules ^{8,9} is reasonably efficient and convenient in use. The method of IR luminescence is applied to study the parameters of vibration-excited molecular gas in the discharge chamber of a process CO₂-laser. The aims of this investigation are:

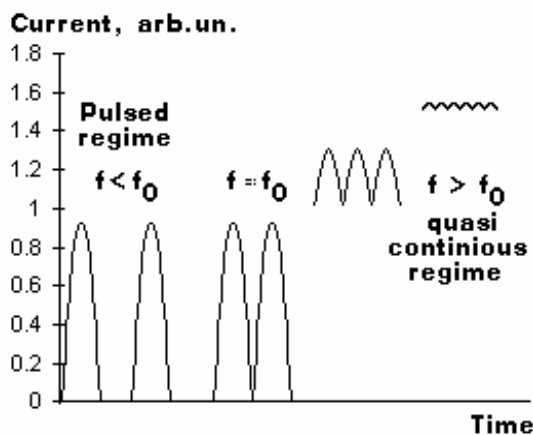


Fig.6. Shape of the discharge current at the inverter various frequencies. $f_0=1/T=1250$ Hz.

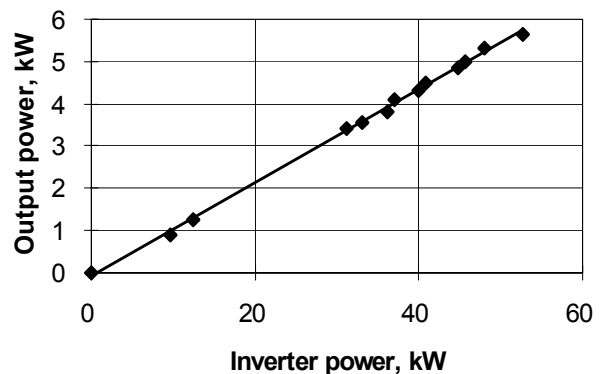


Fig.7 Laser beam power as a function of the power consumed by the power source.

to study the IR luminescence spectra and the parameters of vibration-excited molecular gas of the CO₂ laser active medium; the distribution of vibrational excitation of CO₂ molecules in the GDC volume;

to analyze the possibility of laser output power control by measuring the intensity of IR luminescence of CO₂ molecules from the gas-discharge chamber and to find out the ways of optimization of the electrode system structure and the resonator scheme.

The method of IR luminescence (IRL) diagnostics of CO₂-laser active medium consists in solving an inverse problem for determination of vibrational temperatures of the combined T₁₂ and asymmetric T₃ modes, using the experimentally measured luminescence intensities over the bands of vibrational-rotational transitions of CO₂ molecules in the regions 2.7μm and 4.3μm. Therewith, a set of nonlinear equations is solved, that is the basis for finding out the desired vibrational temperatures:

$$\begin{cases} I_{4.3}^{th} \cdot (T_{12}, T_3, T) - T_{4.3}^{ex} = 0 \\ I_{2.7}^{th} \cdot (T_{12}, T_3, T) - T_{2.7}^{ex} = 0 \end{cases} \quad (1)$$

T_{4.3}^{ex}, T_{2.7}^{ex} are the experimental values of IRL, I_{2.7}th, I_{4.3}th are the rated values of IRL intensity over the bands 2.7μm and 4.3μm as functions of vibrational temperatures T₁₂, T₃ and gas temperature T.

The intensities of IR luminescence over the involved bands of CO₂ molecules vibrational-rotational transitions are evaluated by summing the radiation intensities at some individual transitions of these bands. When calculating IR luminescence from the volume of excited molecular gas, the effect of radiation capture at the resonant vibrational-rotational transitions is taken into account. In our case, the layer of gas wherein the radiation propagates may be represented as a sequence of uniform layers, that simplifies substantially the problem. The experimental values of IR luminescence intensity can be found out from the photodetector signal amplitude at some known values of its spectral sensitivity. The intensities of IR radiation obtained by calculation are compared with those measured experimentally by the use of the set of equations (1), the solution of which gives the desired values of the parameters of vibration-excited molecular gas CO₂, i.e. T₁₂ and T₃. The set of nonlinear equations was solved numerically.

Fig.8 presents schematically the experimental setup. IR luminescence from the discharge region was observed through the output windows made of KCl and located on the sides of GDC in two mutually perpendicular directions: along and transverse the gas flow. The spacing between the chamber output windows and the discharge active area was from 30 cm to 50 cm in different procedures of measurement. Thus, radiation from the discharge area passed through the layer of cold gas identical in its composition, that partially absorbed this radiation.

To register IR radiation and to study its spectrum, an IR spectrofluorimeter (ISF) was developed that consisted of objective, tunable filter, photodetector, registering apparatus (Fig.8). The spatial resolution and high selectivity of the directivity diagram were provided by the long-focus objective (f=50 cm) with a small aperture ratio 1:25. The gas radiation from the GDC volume was converged by the objective from the narrow area that was extended along the optical axis of the ISF and had 6x11 mm² cross-section. For a spectral element, the ISF employed a tunable interference ring filter having the working area λ = 2-8 μm (two segments Δλ₁=2-4.3 μm, Δλ₂ = 3.9 -8 μm), the spectral resolution Δλ/λ = 0.02.

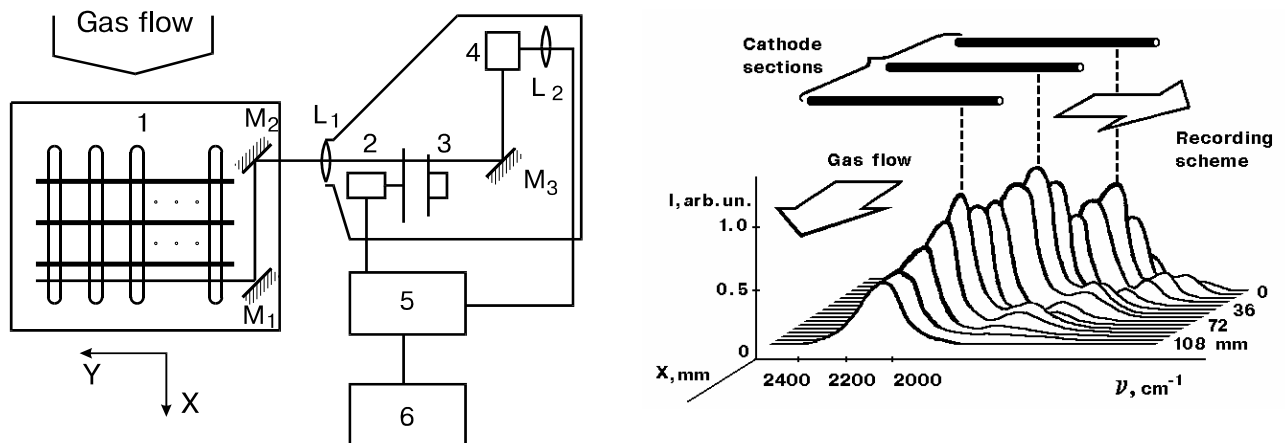


Fig. 8. The scheme of detection of IR luminescence. 1- the gas discharge chamber, 2- the obturator, 3-the tunable IR filter, 4- the IR detector, 5- the synchronized detector, M_1 - M_3 mirrors, L_1 - L_2 lenses.

Fig. 9. Spatial evolution of IR luminescence spectrum along the gas flow.

The filter calibration was performed. The linear dependence of the filter transmission wavelength on the rotation angle provided the precise measurement of IR luminescence spectrum throughout the working range. For the detectors of IR radiation, the ISF employed the photoresistors InSb (in the area $\lambda=2-5.5 \mu\text{m}$) and HgCdTe (in the area ($\lambda=4-8 \mu\text{m}$) cooled by liquid nitrogen. The IR radiation was modulated by the obturator with $f=1\text{kHz}$ frequency. The modulated signal taken from the photodetector was registered by the selective amplifier tuned to the modulation frequency.

To align the optical path and to trace the optical axis in the GDC volume, a He-Ne laser operating at $\lambda=0.63 \mu\text{m}$ and $3.39 \mu\text{m}$ was used. The calibration was performed by registration of radiation from the "black body" source with the irradiate spectral properties known at the specified temperature. In the experiments, the spectrum of IR luminescence from the gas discharge area of CO_2 laser was analyzed depending on the gas mixture composition and laser operation modes; the spatial distribution of vibration-excited CO_2 molecules in the GDC volume was studied and the relation of this distribution to the electrode system structure was determined.

Fig.9 shows the typical spectrum of IR luminescence obtained at the gas mixture composition $\text{CO}_2:\text{N}_2:\text{He} = 1:10:15$, the total pressure in the chamber was $p=26$ Torr and the average current was 15 A. The spectrum has two peaks; a higher one is located in the area $\lambda=4.42\mu\text{m}$ and is due to CO_2 molecules luminescence. The second peak in the spectrum having its center at $\lambda=5\mu\text{m}$ is caused by radiation of CO gas molecules; the equilibrium concentration of this gas under typical CO_2 laser operation can reach 50% of CO_2 initial concentration. At some specific compositions of gas mixture in the spectrum region $\lambda=4.5-5.3\mu\text{m}$ the IR luminescence of the molecules of nitrogen oxides NO, N_2O , NO_2 , as well as ozone molecules O_3 can manifest itself. In the course of studying the spatial structure of gas discharge, the IFL signal was registered from plasma volume in the directions X, Y and Z (the anode-to-cathode direction)

Fig.10 illustrates typical dependencies of IRL on X coordinate, along the gas flow. The modulation of signals is observed, that is related to spatial structure of gas discharge and is determined by the period between cathodes.

The calculation of vibrational temperatures was performed using signals over the bands 4.3 and $2.7\mu\text{m}$ of CO_2 molecules, the gas mixture heating from 300°K at the GDC inlet to 400°K at the GDC outlet was therewith taken into account. The results of calculation of the spatial structure of distribution of vibrational-rotational temperatures T_{12} , T_3 are presented in Fig.10. It is evident that modulation manifests itself only for T_3 , while T_{12} remains constant.

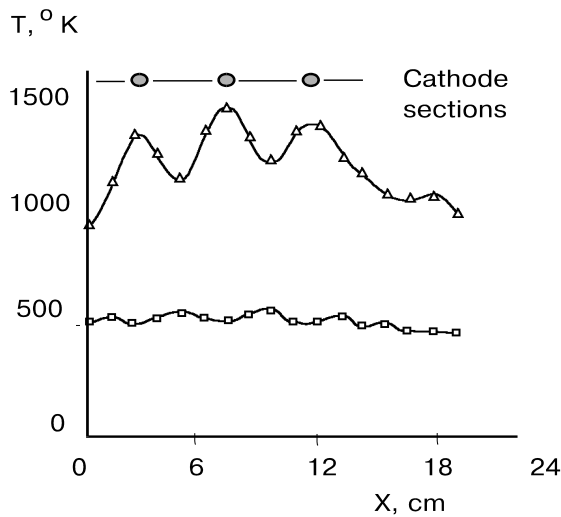


Fig.10. The spatial structure of distribution of vibrational-rotational temperatures T_{12} (the lower curve), T_3 (the upper curve).

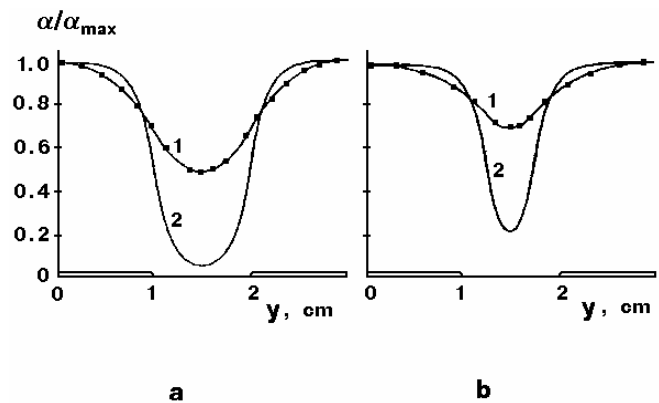


Fig. 11. The experimental points and calculated small signal gain near the anode section surface (a) and in the middle of the discharge gap (b). The curves 1 take into account turbulence diffusion; the curves 2 are for the usual molecular diffusion.

To estimate the efficiency of discharge filling of the interelectrode region, the spatial distribution of IRL transverse the gas flow was studied. Fig.11 illustrates the IRL intensity dependence on Y coordinate at two positions of the observation axis between the electrodes (two values of Z coordinate). As Fig.11 shows, on shifting the optical axis of the system from the cathode to the anode the IRL signal modulation is observed, the period of which corresponds to that of anode sections location.

Modulation is practically lacking close to the cathode, and it increases on shifting the observation axis to the anode, reaching 50% in the vicinity of the anode. At the same time, in the vicinity of the anode the IRL intensity is other than zero in the intervals between the anode sections, though the discharge current is lacking there. The leveling of concentration of the excited CO_2 molecules in the direction of Y axis in the vicinity of the anode is governed by the of diffusion of the excited nitrogen molecules from the discharge area to the region between the anode sections. This process is determined by the turbulence diffusion not by the usual molecular diffusion¹⁰, as we can see in Fig.11.

The correlation of the laser output power with the IRL intensity of CO_2 molecules was measured. Fig.12 illustrates variation of the IRL spectrum over the band $\lambda=4\text{-}5.5\mu\text{m}$ on "switching" the laser resonator. The IRL amplitude falls, but the spectrum pattern does not change therewith. This is associated with the decrease in population of vibrational states of ν_3 mode of CO_2 molecules and with the related vibrational energy exchange of the states of CO molecules at the cost of laser generation at $00^0_1 \rightarrow 10^0_0$ transitions. The joint measurements of CO_2 laser output power and IRL intensity were conducted over the band $4.3\mu\text{m}$ under the resonator detaining condition (Fig.12). The linear decrease of IRL intensity is observed with radiation output power growth (the resonator Q-factor increase). Approximating the linear dependence to the zero signal of luminescence, we obtain the estimate of output power upper limit that can be achieved for the given geometry of the process laser. In our case, this estimate results in 3.5kW power; at the mean power of energy input into the discharge $\sim 25\text{kW}$ the efficiency is $\sim 14\%$. So it can be concluded that the use of the discussed GDC with crossed segmented electrodes in combination with the new laser supply system will permit to achieve the limits of efficiency under optimization conditions.

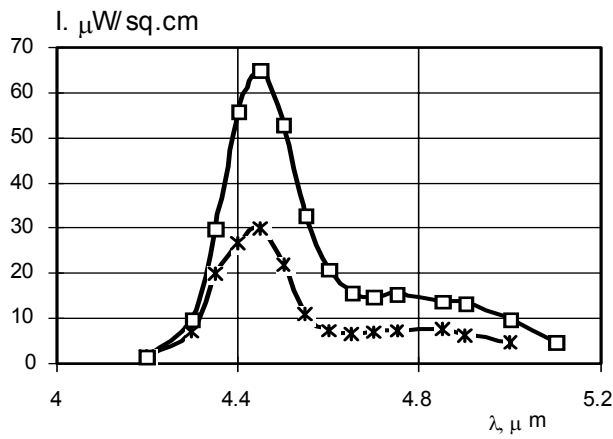


Fig.12. The spectrum of IR radiation of the discharge in the band 4-5.2μm at the switched on (lower curve) and switched off (upper curve) resonator.

5. 2D NUMERICAL MODEL OF SECTIONALIZED DISCHARGE

To perform the numerical experiments, a two-dimensional mathematical model of physical processes in the active medium of an industrial CO₂-laser with multi-sectionalized cathode has been developed¹². The distinctive feature of this model is the self-matching solution of the problems of sectionalized glow discharge, gas dynamics and vibrational kinetics. The model gives an opportunity to obtain the distributions of electrical parameters, namely, current density, E/n (E - is electric field intensity, n - is particles concentration); charged particles density, potential; energy input density in the positive column; kinetic parameters: laser levels population, vibrational temperatures of modes, small signal gain.

The positive column of the discharge was considered, and the assumption of plasma quasineutrality was used. The velocities of processes involving electrons were calculated as a function of E/n . In setting up the equations of charged particles balance it was assumed that the processes of electron attachment to molecule are mainly compensated by disattachment. In the equations the diffusion processes were taken into account, that is important for the case of discharge segmentation. As the electrical circuit included ballast resistors, the equations for the external circuit were used, which connected the currents in the sections. The gas heating was calculated from the gas dynamics equations, the energy equation that took account of energy from V-T relaxation and heat transfer by heat conduction was ignored, as this component was relatively small. An assumption on pressure constancy was taken. The velocities of vibrational levels population were calculated by the known temperature model for CO₂-laser mixture.

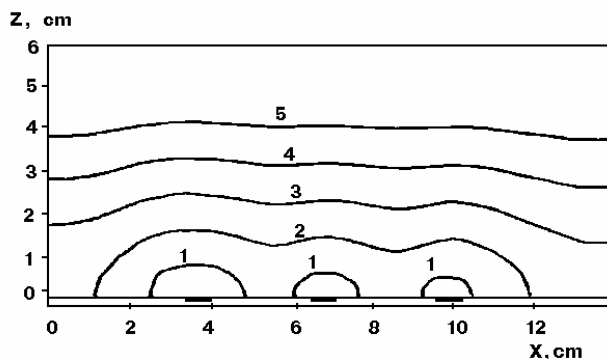


Fig.13. Equipotential lines $\phi=Const$. They are numbered in the increasing order.

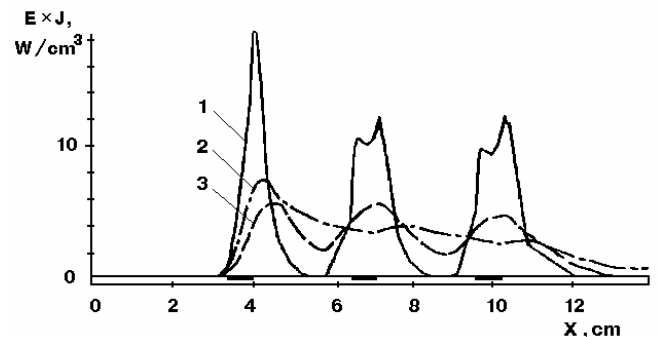


Fig.14. The density of input power along the gas flow. 1- near the cathode, 2- in the middle of the gap, 3- near the anode.

The set of equations describing the model of discharge in the gas flow mixture includes: equations of charge motion and energy conservation in gas, Poisson equation for determination of field intensity, equations of state and vibrational kinetics. The non-stationary equations of charged particles transfer present the balance of electrons and ions. It is evident from the continuity equation for current that the main input into the current is made by the drift of charges in the field. In the equation of energy conservation heat removal by heat conduction and radiation are ignored because of their insignificance. The kinetic model refers to double-mode and three-temperature ones. It is characterized by: T - gas temperature; T_2 - vibrational temperature of the first combined mode ($n00+0k0$) CO_2 ; T_3 - total vibrational temperature of the asymmetric mode CO_2 ($00m$) and N_2 ($v=1$). The variation of the quantum number in each of the modes is determined by excitation, de-activation of vibrations, intermode $V-V^*$ exchange, convective removal.

In the program structure two self-matched sections can be distinguished, namely, the discharge and kinetic ones. The calculation peculiarity is that the discharge section is the first to be calculated, and heat release at the cost of vibrational relaxation is not taken into account in the energy equation. The section of vibrational kinetics is calculated with regard for the found out distribution of power input into the discharge. Then the two sections are jointly calculated, and the discharge section is recalculated with account for the kinetic one. In the calculated variant that is discussed below the following parameters of the model were specified: applied voltage 2400 V; gas flow velocity 100 m/s; discharge gap 6 cm; gas pressure 40 Torr, gas mixture $CO_2:N_2:He=1:6:12$.

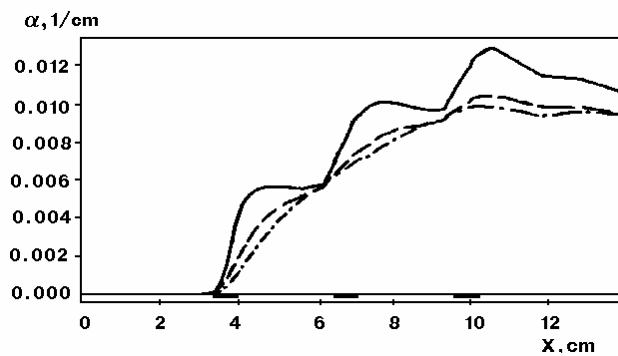


Fig.15. The distributions of the small signal gain along the gas flow direction for three Z coordinates.

From the downstream distribution of potential in the vicinity of the cathode it is clear that the potential grows along the sectionalized cathode. In this case the discharge voltage falls, that is the result of ionization increase. The isolines of charged particles concentrations and current density have the form of the plume extended along the flow and related to the cathode. The isolines of potential are curved near the cathode and around each section (Fig.13). The field intensity distribution at the anode in the sectionalized discharge is slightly non-uniform. The lines of discharge currents become narrower near the cathodes and expand in the direction of the anode extending along the flow. The non-uniformity of current density distribution weakens rapidly away from the segmented cathode to anode. One of the most interesting characteristics of the discharge is the density of input power. It is presented in Fig.14.

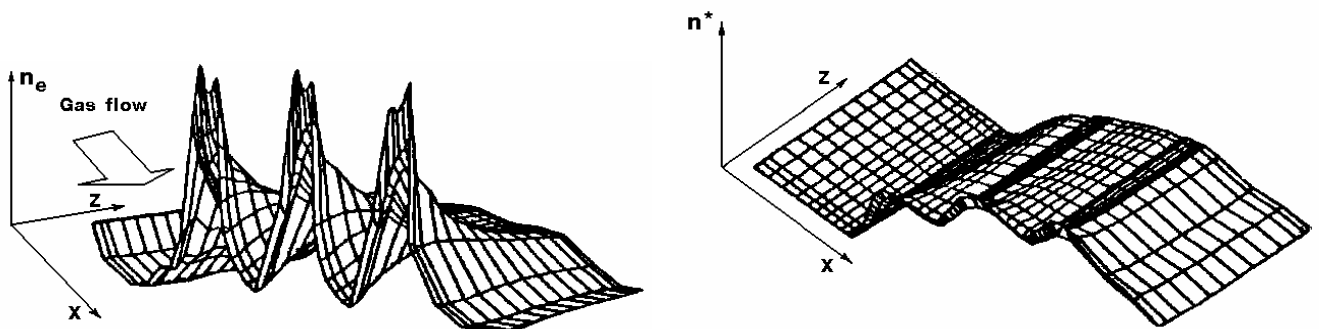


Fig.16. The spatial distribution of the charge density with the switched on preionizer.

Fig.17. The spatial distribution of upper laser level population.

The combined solution of the problems of discharge and kinetics of radiation levels gave an opportunity to follow their mutual influence. There is some correlation between medium excitation and non-uniform distributions of electrical parameters (discharge concentration, power input) related to the cathode sectionalization. This is also confirmed by the experiments on IR luminescence diagnostics of vibrational states of gas molecules in the discharge of industrial sectionalized electrode laser. The distributions of small signal gain are shown in Fig.15. It is evident that sensitivity of distributions from the cathode sections becomes weaker away from the cathode to anode.

In our case, only a small portion of reserved vibrational energy has the time to contribute to translational degrees of freedom. This energy is $\sim 15\%$ with respect to that transformed to heat at the cost of elastic collisions of molecules.

The numerical studies of preionization influence upon the discharge characteristics have been performed. The preionizer was placed along the flow at the distance that was comparable to the discharge gap, as is usually done in prototypes of industrial lasers.

With increase of the density of electrons produced by the preionizer, the profile of charge concentration in the discharge and the energy input become more filled and uniform, (Fig.16). This gives an opportunity to build-up the power input without loss in discharge stability. Fig.9 presents the distribution of intensity of IR luminescence over the band $4\text{...}5\mu\text{m}$ along the gas flow of industrial CO_2 -laser. This signal carries a direct information on population of the upper laser level, as well as on its vibrational temperature T_3 . It is evident that the population of the upper laser level is sensitive to the discharge chamber geometry. As the result of our calculation, the analogy in distributions is seen (Fig.17). We can speak of small signal gain (α) saturation in the discharge chamber of 10 cm length under consideration at mixture pressure $p=40$ Torr; the α maximum value in the discharge gap was therewith $1.4\% \text{ cm}$. With increase of mixture pressure p , the length of vibrational energy relaxation is reduced and the limiting energy input resulting in α saturation falls off.

CONCLUSION

- It is proved, that in transversal fast flowing conception with cross electrode system a large number of individual discharges can be effectively stabilized despite of a small number of electrode sections.
- The described pumping system using sectionalized electrodes and unballast power supply is comparatively simple, effective and cheap. It can be effectively used in the most powerful TE lasers. The laser has pulse periodic and CW regimes of pumping and generation.
- The distribution of the small signal gain is more homogeneous in comparison with discharge structure because of the gas flow and turbulence diffusion.
- , The greater portion of the discharge burns in the recombining plasma under reduced E/n , that has a positive effect upon the discharge stability.

REFERENCES

1. Uwe Habich, Keming Du, Dietmar Ehrlichmann et al. "Development of an Industrial CO_2 -Laser with more than 40kW Output Power: Recent Results", Proc. of X Int. Symp. Gas Flow and Chemical Lasers 1994, pp. 20-24.
2. H.G.Wegmann, P.F.Scheywaerts Proc. 6-th Int. Conf. on Lasers Manufacturing. Birmingham, UK, 1989. Ed. Prof. W.M.Steen IFS-Publication, Springer-Verl, p.59, 1989.
3. N.Tabata, H.Nagai, H.Yoshida et al. "High Power Industrial CO_2 - Lasers", Gas Flow And Chem. Lasers. Proc. of the 5th Int. Symp., Oxford, 20-24 August, pp.1-6, 1984.
4. H.J.J. Seguin, K.H.Nam, J.Dow, V. Seguin. Applied Optics **20**, 13, p.2233, 1981.

5. G.A.Abil'siitov., A.I.Bondarenko, V.V.Vasiltzov et.al. Soviet Journal of Quantum Electronics, **17**, №6, pp.672-676, 1990.
6. L.D. Landau, E.M. Lifshits. Electrodynamics of Continuum. Nauka, Moscow, USSR, 1982.
7. V.G.Niziev, V.N.Kortunov, O.A.Novodvorskii, R.Ya.Sagdeev "Gas Discharge CO₂-Laser with New Pumping System", Plasma Devices and Operations №5, pp. 89-94, 1992.
8. O.A.Achasov, N.N.Kudryavtsev, S.S.Novikov, R.I.Soloukhin, N.A.Fomin. "Diagnostics of Non-Equilibrium States in Molecular Lasers", (in Russian). Minsk, "Nauka i tekhnika", 1985.
9. L.P.Bakhir, V.V.Elov, O.M.Kiselev et al. Soviet J of Quantum Electronics **15**, 1, 1988.
10. M.G.Galushkin, V.S.Golubev, V.E.Zavalova, O.A.Novodvorskii, V.Ya. Panchenko (in Russian) Kvantovaya elektronika, **22**, 5, pp.485-487, 1995.
11. V.M.Gordienko, A.P.Kubishkin, V.Ya.Panchenko, "Physical Basis of Laser And Beam Technology", (in Russian) Moscow, VINITI, **2**, p.74, 1988.
12. V.E.Zavalova, V.I.Ledenev, V.Ya.Panchenko, Yu.P.Raizer, S.T.Surjikov, "Numerical Investigation of Processes in Positive Column of Multi-Sectionalized Diacharge in Fast Flowing Industrial CO₂-laser", Book of Preprints by NICTL, Shatura, Russia 1991, pp. 141-174.